Ansell, G. B., Eds.) Vol. 4, pp 359–434, Elsevier, Amsterdam.
Sillén, L. G., & Martell, A. E. (1971a) *Spec. Publ.—Chem. Soc. No. 17.*
Sillén, L. G., & Martell, A. E. (1971b) *Spec. Publ.—Chem. Soc. No. 25.*
Sudnick, D. R. (1979) Ph.D. Thesis, The Pennsylvania State University, University Park, PA.
van Dam-Mieras, M. C. E., Slotboom, A. J., Pieterson, W. A., & de Haas, G. H. (1975) *Biochemistry 14*, 5387–5393.
van Scharrenburg, G. J. M., Puijk, W. C., Egmond, M. R., de Haas, G. H., & Slotboom, A. J. (1981) *Biochemistry 20*, 1584–1591.
van Wezel, F. M., & de Haas, G. H. (1975) *Biochim. Biophys. Acta 410*, 299–309.
van Wezel, F. M., Slotboom, A. J., & de Haas, G. H. (1976) *Biochim. Biophys. Acta 452*, 101–111.
Verheij, H. M., Volwerk, J. J., Jansen, E. H. J. M., Puijk, W. C., Dijkstra, B. W., Drenth, J., & de Haas, G. H. (1980) *Biochemistry 19*, 743–750.
Volwerk, J. J., & de Haas, G. H. (1982) in *Lipid-Protein Interactions* (Jost, P. C., & Griffith, O. H., Eds.) Vol. 1, pp 69–149, Wiley, New York.
Volwerk, J. J., Dedieu, A. G. R., Verheij, H. M., Dijkman, R., & de Haas, G. H. (1979) *Recl. Trav. Chim. Pays-Bas 98*, 214–220.
Wells, M. A. (1974) *Biochemistry 13*, 4937–4942.
Woyski, M. M., & Harris, R. E. (1963) in *Treatise on Analytical Chemistry* (Kolthoff, I. M., & Elving, P. J., Eds.) Part 2, Vol. 8, p 58, Academic Press, New York.

Influence of Cofactor Pyridoxal 5′-Phosphate on Reversible High-Pressure Denaturation of Isolated β_2 Dimer of Tryptophan Synthase Bienzyme Complex from *Escherichia coli*†

Thomas Seifert, Peter Bartholmes,‡ and Rainer Jaenicke*

Institut für Biophysik und Physikalische Biochemie, Universität Regensburg, D-8400 Regensburg, FRG
Received July 2, 1984

ABSTRACT: High hydrostatic pressure has been shown to cause reversible dissociation of the isolated apo β_2 dimer of tryptophan synthase from *Escherichia coli* into enzymatically inactive monomers [Seifert, T., Bartholmes, P., & Jaenicke, R. (1982) *Biophys. Chem. 15*, 1–8]. Addition of the coenzyme pyridoxal 5′-phosphate affects the structural stability, as well as the kinetics of dissociation and deactivation. The apo β_2 dimer is deactivated faster than the holoenzyme by a factor of 10. The midpoints of the corresponding equilibrium transition curves are observed at 690 and 870 bar, respectively. As shown by hybridization of native and chemically modified β chains, the loss of enzymatic activity is accompanied by subunit dissociation. An additional deactivating effect is produced by the pressure-induced release of the cofactor from the holoenzyme. Renaturation after decompression has been monitored by circular dichroism and intrinsic fluorescence emission. Alterations of the dichroic absorption at 222 nm reflect the recovery of the native secondary structure, while tryptophan fluorescence represents a specific probe for the native tertiary structure in the immediate neighborhood of the active center of the enzyme. By application of both methods to monitor the reconstitution of the apo β_2 dimer, two first-order processes may be separated along the time scale. The faster phase ($k_1 = 1.2 \times 10^{-2}$ s^{-1}) yields a "structured monomer" with 85% native secondary structure and the tryptophan side chain buried in its native hydrophobic environment. As indicated by sodium borohydride reduction, this intermediate is able to interact with the coenzyme pyridoxal 5′-phosphate in the correct way; however, it does not show enzymatic activity. During the second phase ($k_1' = 8.3 \times 10^{-4}$ s^{-1}), a slow reshuffling process provides properly folded contact regions for rapid dimerization of the inactive monomers resulting in the catalytically active native holoenzyme.

The biological function of proteins (enzymes) depends on the unique spatial arrangement of their polypeptide backbone. This gains its stability from noncovalent short-range and long-range forces including hydrogen bonds, ion pairs, and hydrophobic interactions. Experiments making use of reversible denaturation and reconstitution (Anson, 1945; Anfinsen et al., 1961) clearly show that the one-dimensional amino acid sequence contains the "code" for the three-dimensional folding of the polypeptide chain in its aqueous or nonaqueous environment. The underlying folding mechanism involves an ordered sequence of steps proceeding from short-lived microdomains to increasingly higher substructures, which finally undergo tertiary structure formation due to long-range interactions between preformed elements of secondary structure. The time scale for the various intermediate states on the pathway of folding ranges from microseconds (helix formation) to minutes ("reshuffling") (Ko et al., 1977; Baldwin, 1980; Weaver, 1982; Burns & Schachman, 1982; Jaenicke, 1984).

The reconstitution of oligomeric proteins includes specific homologous or heterologous interactions of protein subunits. Since it requires the correct formation of subunit contact regions, association reactions must be late events on the

† Dedicated to Professor Max A. Lauffer on the occasion of his 70th birthday. This work was supported by grants of the Fonds der Chemischen Industrie and the Deutsche Forschungsgemeinschaft to P.B. and R.J.
‡ Present address: Institut für Physiologische Chemie, Universität Witten-Herdecke, D-5810 Witten, FRG.

0006-2960/85/0424-0339$01.50/0

pathway of the formation of native protein assemblies (Jaenicke, 1983a, 1984). In contrast to the unimolecular characteristics of folding reactions, quaternary structure formation contains bimolecular steps that may or may not be rate limiting in the overall process of reconstitution (Jaenicke, 1974, 1984; Jaenicke & Rudolph, 1983; Zabori et al., 1980; Jaenicke & Perham, 1981).

Ligands, like cofactors or substrates, are used to stabilize the native structure of a given protein. They may also influence the kinetics of reconstitution by accelerating rate-limiting steps or by stabilizing folding intermediates and/or the final product of reconstitution (Jaenicke, 1984).

Detailed studies on NAD-dependent dehydrogenases have shown that the coenzyme, NAD^+ or NADH, and the substrate do not exhibit a significant influence on the reconstitution of lactate dehydrogenase (Rudolph et al., 1977), malate dehydrogenase (Jaenicke et al., 1979), and pyruvate dehydrogenase (Jaenicke & Perham, 1981) while in the case of glyceraldehyde-3-phosphate dehydrogenase a 10-fold enhancement of the rate of folding has been reported after covalently linking an NAD analogue to the enzyme (Jaenicke et al., 1980).

In the case of the pyridoxal 5′-phosphate dependent tryptophan synthase from *Escherichia coli* (EC 4.2.1.20), the covalent attachment of the cofactor is the natural state of the holoenzyme. The isolated β_2 "subunit" of the $\alpha_2\beta_2$ bienzyme complex has been extensively studied with respect to its denaturation–renaturation properties (Groha et al., 1978; Goldberg & Zetina, 1980; Zetina & Goldberg, 1980; Seifert et al., 1982). The protein is an extremely stable dimer. It catalyzes the reaction

$$\text{indole} + \text{L-serine} \rightarrow \text{L-tryptophan} + H_2O \qquad (1)$$

and can be reversibly denatured and dissociated at high hydrostatic pressure (Seifert et al., 1982) or in the presence of 4 M guanidine hydrochloride at acid pH (Groha et al., 1978). In the present study, we investigate the role of pyridoxal 5′-phosphate as a positive effector of structural stability on the high-pressure denaturation of the enzyme.

Materials and Methods

Tryptophan synthase β_2 subunit was purified from the A2/F′A2 mutant strain of *Escherichia coli* (kindly donated by Drs. C. Yanofsky and I. P. Crawford) and stored frozen at −75 °C (Bartholmes et al., 1976). Pyridoxal phosphate was purchased from Serva (Heidelberg) and dithioerythritol from Roth (Karlsruhe). All other chemicals were of A-grade purity from Merck (Darmstadt). Quartz-bidistilled water was used for making up solutions.

If not stated otherwise, all experiments were performed in the following buffer: 0.1 M triethanolamine hydrochloride (pH 7.8 at 10 °C), 0.1 M NaCl, 2 mM dithioerythritol, 0.5 mM ethylenediaminetetraacetic acid (EDTA). This buffer reveals an excellent pH stability with respect to high hydrostatic pressure (Neumann et al., 1973); morever, it does not interact with pyridoxal phosphate to yield an unproductive Schiff base. Buffer and protein solutions were stored under nitrogen.

Apo β_2 subunit was prepared by passing holoenzyme through a small band of 0.5M hydroxyammonium chloride on a Sephadex G-25 column (0.8 × 25 cm) equilibrated with buffer. The concentration of the β_2 subunit was determined spectrophotometrically from $A_{290nm} = 0.75$ cm^2 mg^{-1} (Kirschner et al., 1975). Enzymatic activity was measured as described previously (Faeder & Hammes, 1970) on a Zeiss DMR 10 spectrophotometer. The activity of the freshly prepared holoenzyme was about 3800 Yanofsky units mg^{-1} or 8 IU mg^{-1}. One Yanofsky unit is defined as the amount of enzyme that catalyzes the conversion of 0.1 μmol of indole to tryptophan per 20 min at 37 °C. Both units may be interconverted on the basis of the known temperature dependence of the specific activity of the enzyme (Seifert, 1980).

Absorbance, fluorescence emission, and circular dichroism spectra were measured on a Zeiss DMR 10 spectrophotometer, a Hitachi Perkin-Elmer MPF 44 A spectrofluorometer, and a Jasco J-500A spectropolarimeter, respectively.

High-pressure quench experiments for the determination of pressure-dependent deactivation and dissociation were performed with autoclaves and pressure-generating equipment as described elsewere (Schmid et al., 1978; Schade et al., 1980; Jaenicke, 1983b). After pressure release, the enzyme solution was immediately removed, and the catalytic activity of the protein was measured under normal pressure at 25 °C as described above. In order to prevent reactivation during the test, the experimental conditions for determining the kinetics of deactivation and reactivation, respectively, had to be varied slightly by adding 10 μg of trypsin (TPCK-treated)/mL of test medium and by lowering the temperature from 37 to 25 °C (Seifert et al., 1982).

Hybridization of β subunits with chemically modified monomers after pressure release was applied to quantify the degree of pressure-induced dissociation. Chemical modification made use of $NaBH_4$ reduction of the internal aldimine linkage between pyridoxal phosphate and Lys-86 in the active center of the enzyme (Crawford et al., 1980; Balk et al., 1981).

To follow the kinetics of dissociation, a 10-fold excess of the (separately pressure-dissociated) reduced β monomers was added to the pressure-dissociated unmodified enzyme at varying times. Reassociation kinetics of the dissociated enzyme were measured as described previously, with a 10-fold excess of reduced β monomers (Seifert et al., 1982). The respective degree of hybrid formation was analyzed by polyacrylamide gel electrophoresis under native conditions and subsequent densitometric analysis of the stained protein bands (Hathaway et al., 1969). Resolution of the denaturing β chains from the cofactor pyridoxal phosphate was traced by $NaBH_4$ fixation of residual internal aldimines after the time intervals given (Balk et al., 1981).

Results

High-Pressure Deactivation and Dissociation of Apo β_2 Dimer. As reported previously (Seifert et al., 1982), the specific activity of the β_2 dimer of tryptophan synthase remains constant for several weeks. This observation, together with the high yield of reactivation and the regain of native characteristics of the reconstituted enzyme, provides optimum conditions for kinetic renaturation experiments.

Figure 1 (left half) shows the time-dependent deactivation of the apoenzyme at different pressures. If one plots the final values after reaching equilibrium vs. pressure, the corresponding equilibrium transition curve is obtained (Figure 1, right half). The data may be analyzed on the basis of a simple dissociation process (cf. Figure 3):

$$\beta_2 \underset{k_{-1}}{\overset{k_1}{\rightleftharpoons}} 2\beta \qquad (2)$$

Writing $[\beta_2^0]$ and $[\beta_2^\infty]$ for the concentrations of the β_2 dimers at zero time and at equilibrium, the actual concentration (activity) at a given time β_2 may be expressed by

$$\beta_2 = \frac{[\beta_2^0]\{[\beta_2^0] + [\beta_2^\infty] \exp(k_1 Q t)\}}{[\beta_2^0] \exp(k_1 Q t) + [\beta_2^\infty]} \qquad (3)$$

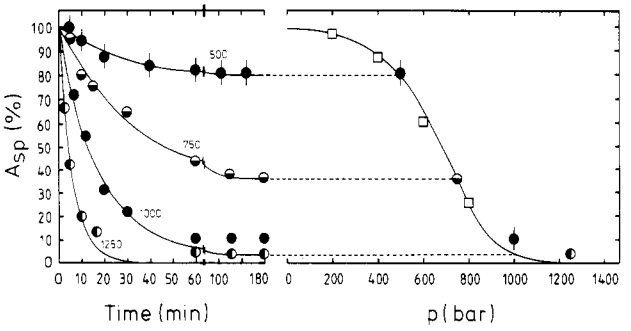

FIGURE 1: Pressure-induced deactivation of the isolated apo β_2 dimer of tryptophan synthase. (Left) Time-dependent deactivation at 10 °C: A_{sp}, specific activity (%); enzyme concentration 0.1 mg/mL (2.3 μM); (slashed solid circle) 500, (◒) 750, (●) 1000, and (◐) 1250 bar. Solid lines calculated according to first-order kinetics with values for k_1 and β_2^∞ collected in Table I. (Right) Equilibrium transition profile: final values after approximately 10 half-times. Symbols are as in the left-hand kinetics; (□) final values measured at additional pressures over the transition range. Solid line calculated according to eq 4 with $K(P_0) = 4.5 \times 10^{-10}$ M as equilibrium constant at normal pressure and $\Delta V = -290$ cm^3 mol^{-1} as reaction volume.

Table I: Pressure Dependence of Individual First- and Second-Order Rate Constants (k_1 and k_{-1}) and Residual Equilibrium Concentrations (β_2^∞) of the β_2 Dimer of Tryptophan Synthase

	P (bar)	k_1 (s^{-1})	k_{-1} (L mol^{-1} s^{-1})	β_2^∞ (%)
apoenzyme	1	1.0×10^{-5a}	1.1×10^{4a}	99
	500	9.5×10^{-5}	2.0×10^{2}	80
	750	28×10^{-5}	2.8×10^{1}	36
	1000	90×10^{-5}	3.7	4
	1250	280×10^{-5}	0.45	0
holoenzyme	1	1.7×10^{-8a}	1.7×10^{8a}	100
	750	770×10^{-8}	5.0×10^{1}	88
	900	3200×10^{-8}	2.3	31
	1000	8500×10^{-8}	2.3×10^{-1}	3
	1250	45000×10^{-8}	1.6×10^{-3}	0

[a] Obtained by extrapolation to zero pressure of the straight lines according to $\ln k = f(P)$ in Figure 2B.

with $Q = ([\beta_2^0] + [\beta_2^\infty])/([\beta_2^0] - [\beta_2^\infty])$ (Seifert, 1983).

The solid transition curve has been calculated according to

$$\ln K_{P,T} = \ln K_{P_0,T} - \frac{\Delta V}{RT}P \qquad (4)$$

Optimum fit was obtained with a dissociation constant at atmospheric pressure $K(P_0) = 4.5 \times 10^{-10}$ M, and the reaction volume $\Delta V = -290$ mL mol^{-1}.

Linearizing the kinetic traces (Figure 2A) yields the individual first-order constants k_1, which allow k_{-1} to be calculated according to

$$k_{-1} = k_1 \frac{[\beta_2^\infty]}{4([\beta_2^0] - [\beta_2^\infty])^2} \qquad (5)$$

The corresponding data, including the final equilibrium values of the reversible deactivation, are summarized in Table I. A half-logarithmic plot of k_1 and k_{-1} vs. pressure (Figure 2B) yields the volume of activation according to the expression

$$\ln k_{1,-1(P,T)} = \ln k_{1,-1(P_0,T)} - P\frac{\Delta V^*_{1,-1}}{RT} \qquad (6)$$

As a result, we obtain $\Delta V^*_1 = -105$ mL mol^{-1} and $\Delta V^*_{-1} = 185$ mL mol^{-1}, confirming the numerical value for the reaction volume according to

$$|\Delta V| = |\Delta V^*_1| + |\Delta V^*_{-1}| \qquad (7)$$

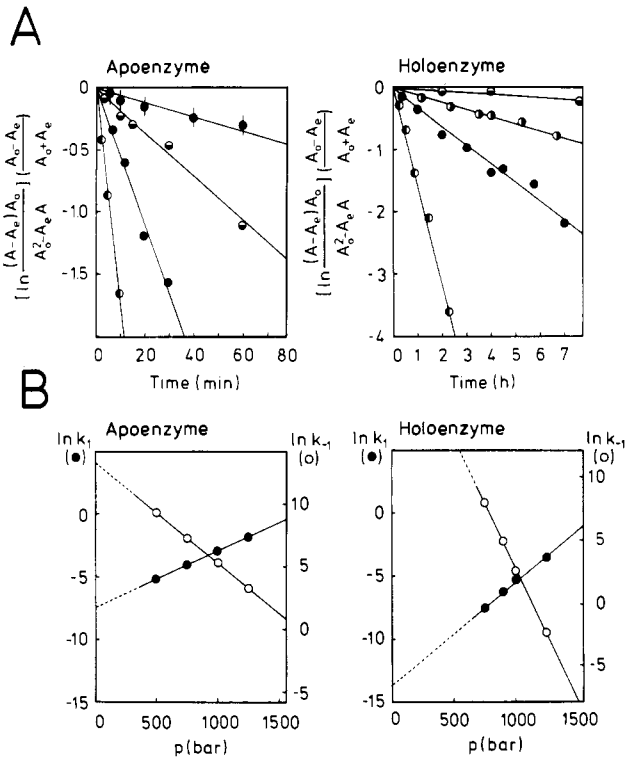

FIGURE 2: Determination of kinetic constants from data given in Figure 1 (apoenzyme) and Figure 4 (holoenzyme). (A) Linearization of the deactivation kinetics according to eq 2 and 3: $\{\ln [([\beta_2] - [\beta_2^\infty])[\beta_2^0]/([\beta_2^0]^2 - [\beta_2^\infty][\beta_2])]\}Q^{-1} = -k_1 t$ with β_2^∞ from Table I. $\beta_2^0 = 100$ and Q is as defined. Symbols are as in Figure 1. (B) Semilogarithmic plot of the rate constants of dissociation (k_1) and association (k_{-1}) (Table I) vs. pressure yielding the activation volumes $\phi\Delta V^*_{1,-1}$ for the forward and backward reaction.

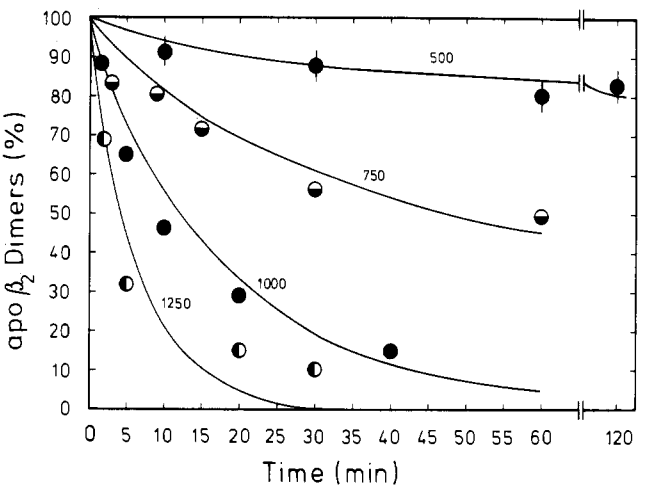

FIGURE 3: Pressure-dependent dissociation of the apo β_2 dimer as monitored by hybridization and subsequent polyacrylamide gel electrophoresis under native conditions. Solid lines represent the corresponding deactivation kinetics.

As taken from hybridization experiments (Figure 3), the kinetics of deactivation are paralleled by dissociation of the β_2 dimer into monomers. The data can be fitted quantitatively with the individual rate constants given in Table I. The final equilibrium values are identical within the limits of error.

Since we cannot exclude that the observed hybridization may result from intermolecular subunit exchange via tetrameric encounter complexes, sucrose gradient centrifugation was used as an independent technique. By application of a 40 000 revolutions/min in a swing-out rotor (r_{max} = 16 cm), a decelerating effect on the sedimentation velocity is observed; the

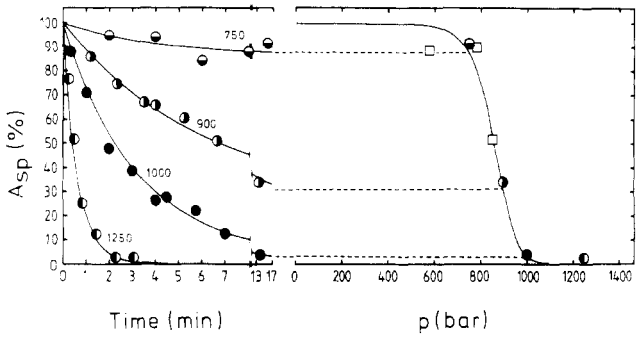

FIGURE 4: Pressure-induced deactivation of isolated holo β_2 dimer of tryptophan synthase. (Left) Time-dependent deactivation at 10 °C: A_{sp}, specific activity (%); enzyme concentration 0.1 mg/mL; buffer supplemented with 40 μM pyridoxal 5'-phosphate; (◒) 750, (◑) 900, (●) 1000, and (◐) 1250 bar. Solid curves are calculated as in Figure 1. (Right) Equilibrium transition profile: final value after approximately 10 half-times. Symbols are as in the left side; (□) final values measured at additional pressures over the transition range.

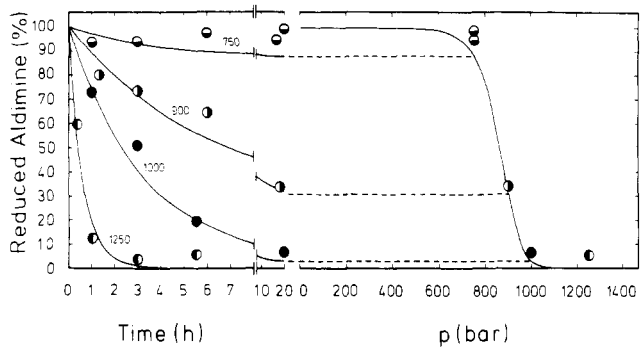

FIGURE 5: Kinetics of resolution of holoenzyme during pressure-induced deactivation as monitored by $NaBH_4$ reduction and subsequent separation of the reduced and unreduced fraction. Solid lines represent the corresponding deactivation kinetics. Experimental conditions and symbols are as in Figure 4.

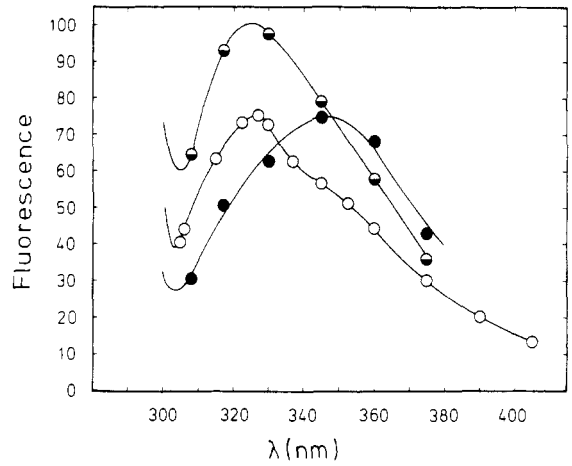

FIGURE 6: Fluorescence emission spectra of native β_2 dimer, denatured β chains, and an intermediate on the pathway of refolding. Excitation wavelength was 295 nm, 10 °C. (○) Native apo β_2 dimer; (●) denatured protein; (◒) folding intermediate. In order to determine the intermediate spectrum, renaturation kinetics were monitored at different emission wavelengths; the profile depicts the fluorescence emission at maximum intermediate concentration (after 5 min; cf. Figure 8).

respective sedimentation coefficients of the enzyme in the top and bottom part of the tubes are 5.3 and 3.3 S, respectively. Dicamelli et al. (1973) reported 5.1 S for the dimer. The hydrostatic pressure where dissociation occurs is close to the midpoint of the equilibrium transition illustrated in Figure 1, thus corroborating the hypothetical dissociation mechanism (Seifert et al., 1984b).

High-Pressure Deactivation and Dissociation of Holo β_2 Dimer. In comparison with the apoprotein, the holo β_2 dimer shows increased stability due to the internal aldimine between the cofactor pyridoxal phosphate and the active center of the enzyme. As shown in Figure 4, the rate of inactivation is slowed down by about 1 order of magnitude, and the midpoint of the equilibrium transition is shifted significantly to higher pressures (870 bar as compared to 690 bar for the apoenzyme). The cooperativity of the transition curve is appreciably higher, in accordance with the large reaction volume $\Delta V = -670$ mL mol^{-1}. To obtain optimum fit of the data, a dissociation constant at normal pressure of $K_{P_0} = 1.2 \times 10^{-17}$ M was assumed.

Again, linearization of the respective kinetics of deactivation is necessary to obtain the individual rate constants k_1 and k_{-1} (Figure 2, Table I). The corresponding activation volumes are $\Delta V^{\ddagger} = -190$ mL mol^{-1} and $\Delta V^{\ddagger}_{-1} = 480$ mL mol^{-1}, respectively.

In order to characterize the pressure denaturation of the holoenzyme in more detail, insight into the interaction of pyridoxal phosphate with the β chain at high pressure is desirable. By using $NaBH_4$ reduction of the productive internal aldimine in the active center of the enzyme, it becomes clear that the protein is completely resolved under the given conditions. Beyond that, the kinetics of resolution may be fitted by the parameters determined for the pressure deactivation of the enzyme (Figure 5). The equilibrium values reached at the indicated pressures turn out to be closely similar. Thus, denaturation of the holoenzyme at high hydrostatic pressure finally generates apo β monomers, since dissociation of the β_2 dimer is facilitated significantly after the detachment of pyridoxal phosphate.

High-Pressure Denaturation of Apo β Subunit. Applying high pressure to the β_2 dimer of tryptophan synthase leads to a significant shift of the wavelength of maximum fluorescence emission from 327 to 345 nm ($\lambda_{exc} = 295$ nm) (Figure 6). Obviously, the only tryptophan residue (Trp-176) present in the β chain is exposed to the aqueous solvent in the course of pressure dissociation.

Reconstitution and Cofactor Binding of Isolated Apo β Chains. Reconstitution of the enzyme after pressure release is an essentially irreversible process leading back to the native state (Jaenicke, 1982). Thus, first-order conformational changes and a second-order association have to be involved as elementary steps. The individual reaction rates of the different processes determine the overall kinetics as well as the mechanism of reconstitution.

As monitored by tryptophan fluorescence and far-UV circular dichroism, the recovery of the native secondary structure is biphasic with well-separated first-order rate constants, $k = 1.2 \times 10^{-2}$ s^{-1} and $k' = 8.3 \times 10^{-4}$ s^{-1} [calculated according to Paul et al. (1980)]. The tryptophan residue must be close to the active site of the enzyme, as indicated by the significant fluorescence energy transfer between tryptophan and pyridoxal phosphate, bound as productive internal aldimine (P. Bartholmes, unpublished data). If one monitors the kinetic traces at different wavelengths, a transitory emission spectrum may be constructed (Figure 6). Its maximum at $\lambda_{max} = 327$ nm clearly indicates that the first rapid phase on the folding pathway generates an intermediate in which the indole moiety of tryptophan (exposed to the solvent under pressure) is already buried in its native hydrophobic pocket. This intermediate reaches its maximum concentration after 5 min (cf. Figure 8). Although it does not exhibit enzymatic activity, it is

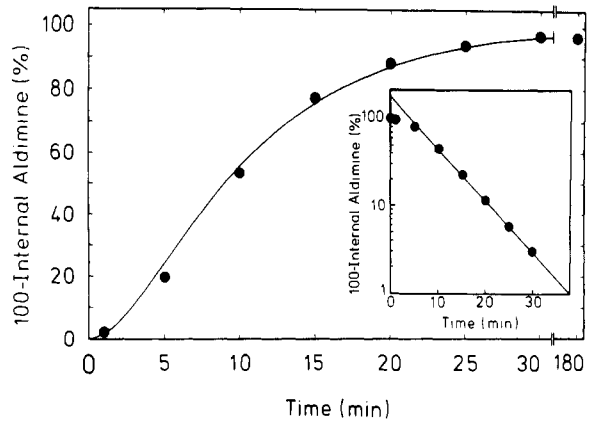

FIGURE 7: Binding of pyridoxal 5′-phosphate during renaturation as monitored by $NaBH_4$ reduction (Balk et al., 1981). (Insert) Semilogarithmic evaluation of the kinetics of ligand binding. Experimental conditions are as in Figure 4. Pyridoxal 5′-phosphate concentration was 0.1 mM.

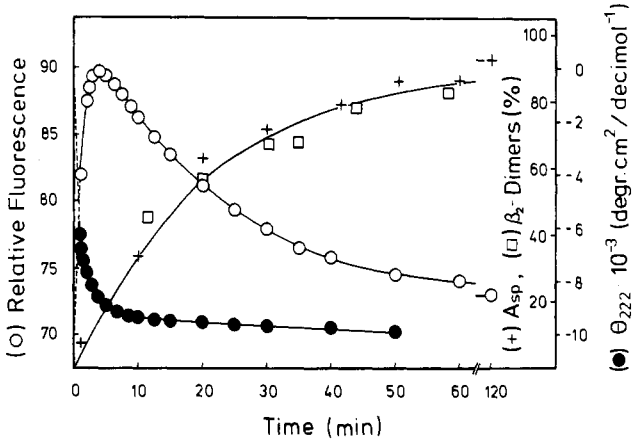

FIGURE 8: Kinetics of renaturation, pyridoxal 5′-phosphate binding, reassociation, and reactivation of pressure-denatured, inactive apo β monomers at 10 °C. Enzyme concentration was 0.1 mg/mL. (●) Molar ellipticity at 222 nm; (○) fluorescence emission at 317 nm (λ_{exc} = 280 nm); (□) reassociation to β_2 dimers; (+) reactivation (A_{sp}, specific activity). Solid lines calculated on the basis of the rate constants for the fast and slow phases: $k_1 = 1.2 \times 10^{-2}$ s^{-1}; $k'_1 = 8.3 \times 10^{-4}$ s^{-1} [cf. Seifert et al. (1982)].

capable of interacting with the coenzyme pyridoxal phosphate to yield the productive internal aldimine. This is clearly shown by polyacrylamide gel analysis after quenching reconstitution with sodium borohydride (Figure 7).

However, not only the active center is reconstructed to a substantial amount, but extensive parts of the overall secondary structure must have been rebuilt since 85% of the original α helicity are found at the end of this rapid initial phase (Figure 8). As shown in a recent publication (Seifert et al., 1982), reassociation and reactivation of the dimeric protein run strictly parallel, this observations being unaffected by concentrations varying by a factor of 100. The respective first-order rate constant correlates with the slow phase of the biphasic renaturation yielding complete reconstitution (>95%) of native enzyme with full catalytic efficiency. The reaction rate determined after pressure release is in good agreement with the respective constant measured for the reconstitution of the enzyme after complete denaturation in 4.5 M guanidinium chloride at pH 2.3 (Groha et al., 1978).

DISCUSSION

The interaction of the α and β_2 constituents in the tetrameric $\alpha_2\beta_2$ bienzyme complex of tryptophan synthase represents an example for the control of both the structure and the catalytic efficiency of an enzyme due to the mutual stabilization of its constituent subunits (Faeder & Hammes, 1971; Kirschner et al., 1975; Weischet & Kirschner, 1976). In the present experiments, the additional influence of the coenzyme pyridoxal phosphate on the structural stability, as well as the kinetics of dissociation and deactivation, has been investigated. The coenzyme is known to form a productive internal aldimine with a lysyl residue (Lys-86) in the active center of the β chain, this way providing optimum efficiency of the enzyme complex (Wiesinger et al., 1979; Crawford et al. (1980).

The interactions operative in maintaining the quaternary structure and the effect on the stability exerted by the binding of small ligands may be understood to some extent if dissociation–association are fully reversible. Generally, subunit dissociation and subsequent reconstitution are perturbed by side reactions such as "wrong aggregation" (Zettlmeissl et al., 1979). In the case of high-pressure deactivation (which is accompanied by dissociation), full reversibility has been observed (Jaenicke, 1983b).

As shown by fluorescence titration measurements with lactate dehydrogenase as a representative example, this is accomplished by conformational changes minimizing the hydrophobic surface area of the subunits in their dissociated state (Müller et al., 1982). The present experiments prove tryptophan synthase to be highly stable toward high-pressure deactivation. Even in the absence of the coenzyme and the α subunit, the β_2 dimer exhibits an exceedingly high pressure of half-deactivation, $P_{1/2}$ = 690 bar. Formation of the productive internal aldimine with the coenzyme results in increased stability, the value of $P_{1/2}$ for the holoenzyme being shifted to 870 bar. Correspondingly, the rates of deactivation observed for the holoenzyme close to the range of transition are found to be smaller by a factor of 10 as compared to that of the apoenzyme. The large negative activation volumes calculated for the deactivation of both the apo- and holoenzymes reflect the drastic increase of the rate of deactivation with increasing pressure.

The dissociation of the β_2 dimer into inactive monomers has been detected and quantitatively determined by making use of hybridization of the native β subunit and the subunit with pyridoxal phosphate covalently linked to Lys-86 by $NaBH_4$ reduction. Obviously, this method cannot unequivocally discriminate pressure-induced dissociation on one hand and subunit exchange by way of encounter complexes consisting of native and chemically modified subunits, on the other.

A pressure-induced increase in the rate of subunit exchange may be excluded because the stabilization of the transition state and the dimeric end product are expected to run parallel. In addition, independent evidence from sucrose gradient centrifugation clearly demonstrates subunit dissociation to take place (Seifert et al., 1984b).

Apart from causing subunit dissociation (which involves only noncovalent intermolecular forces), high hydrostatic pressure resolves the covalent Schiff base between the coenzyme pyridoxal 5′-phosphate and the essential lysyl side chain in the active center of the enzyme. Other pyridoxal 5′-phosphate dependent enzymes have been shown to remain in their holo form even under drastic denaturation conditions (Fasella & Hammes, 1964). In the present case, we are led to assume that the inactive protein generated from the native holo β_2 subunit at pressures beyond 1 kbar comprises the homogeneous apo monomer. Obviously, electrostriction of the (ionized) groups involved in both Schiff base formation and subunit assembly determine the reaction volume. As indicated by

fluorescence labeling experiments using 8-anilinonaphthalene-1-sulfonic acid (ANS), hydrophobic interactions participate in the overall pressure effect (Seifert et al., 1984a). The mechanism involved differs significantly from the one reported previously for the high-pressure deactivation of lactate dehydrogenase where pressure favors coenzyme binding and subunit dissociation without significantly affecting ANS fluorescence (Jaenicke et al., 1979; Müller et al., 1982).

After fast release of pressure, the regain of the native structure of the enzyme occurs in a biphasic reaction. The first phase is characterized by a half-time of about 1 min and leads to a native-like folding intermediate characterized by ~85% of the native helix content; the indole moiety of the only tryptophan residue is no longer exposed to the solvent. Instead, the native hydrophobic pocket is restored, as indicated by the significant blue shift of the maximum of fluorescence emission. Due to the close interaction of the fluorophore with the ring system of the bound coenzyme, this spectral effect may be assumed to reflect conformational changes in the immediate vicinity of the active center of the enzyme. The subsequent second phase may be attributed to a slow reshuffling process generating the structured monomer. Diffusion-controlled dimerization then yields the catalytically active β_2 dimer in its native state.

Although the above-mentioned intermediate is enzymatically inactive, it shows at least part of the structural and functional properties of the active site of the enzyme. As shown by reductive quench experiments (using $NaBH_4$), the coenzyme is recognized by the one specific lysyl residue (Lys-86) in the N-terminal folding domain of the β subunit (Högberg-Raibaud & Goldberg, 1977); the remaining 17 lysyl residues are not involved in the reaction.

In accordance with results reported by Goldberg & Zetina (1980), it can be assumed that the first (rapid) phase described in this paper reflects the folding of the F_1 domain. Evidence comes from the observed change in the intrinsic fluorescence that monitors the transfer of the only tryptophan residue present in the whole β chain into the hydrophobic interior of the F_1 domain. The second (slower) phase may be assumed to belong to the slow reorientation of the two structural domains, F_1 and F_2. The reshuffling of these domains provides the correctly oriented contact regions for both the dimerization and the rearrangement of the active center, which are required to yield the functional pattern of the noncovalent contacts between the enzyme on one hand and the substituents of the pyridine ring of the coenzyme molecule on the other.

Acknowledgments

Skillful technical assistance by Brigitte Teuscher is gratefully acknowledged. We thank Drs. M. R. Kula and K. Kieslich, GBF Stöckheim, for their generous help in growing bacteria on a large scale.

Registry No. EC 4.2.1.20, 9014-52-2; pyridoxal 5'-phosphate, 54-47-7.

References

Anfinsen, C. B., Haber, E., Sela, M., & White, F. H. (1961) *Proc. Natl. Acad. Sci. U.S.A. 47*, 1309–1314.

Anson, M. L. (1945) *Adv. Protein Chem. 2*, 361.

Baldwin, R. L. (1980) in *Protein Folding* (Jaenicke, R., Ed.) pp 369–385, Elsevier/North-Holland, Amsterdam and New York.

Balk, H., Frank, A., Bartholmes, P., & Jaenicke, R. (1981a) *Eur. J. Biochem. 121*, 105–112.

Bartholmes, P., Kirschner, K., & Gschwind, H.-P. (1976) *Biochemistry 15*, 4712–4717.

Burns, D. L., & Schachman, H. K. (1982) *J. Biol. Chem. 257*, 8648–8654.

Crawford, I. P., Nichols, B. P., & Yanofsky, C. (1980) *J. Mol. Biol. 142*, 489–502.

Dicamelli, R. E., Balbinder, E., & Lebowitz, J. (1973) *Arch. Biochem. Biophys. 155*, 315–324.

Faeder, E. J., & Hammes, G. G. (1970) *Biochemistry 9*, 4043–4049.

Faeder, E. J., & Hammes, G. G. (1971) *Biochemistry 10*, 1041–1045.

Fasella, P., & Hammes, G. G. (1964) *Biochemistry 3*, 530–535.

Goldberg, M. E., & Zetina, C. R. (1980) in *Protein Folding* (Jaenicke, R., Ed.) pp 469–484, Elsevier/North-Holland, Amsterdam and New York.

Hathaway, G. M., Kida, S., & Crawford, I. P. (1969) *Biochemistry 8*, 985–997.

Högberg-Raibaud, A., & Goldberg, M. E. (1977) *Proc. Natl. Acad. Sci. U.S.A. 74*, 442–446.

Jaenicke, R. (1974) *Eur. J. Biochem. 46*, 149–155.

Jaenicke, R. (1982) *Biophys. Struct. Mech. 8*, 231–256.

Jaenicke, R. (1983a) in *Mobility and Recognition in Cell Biology* (Sund, H., & Veeger, C., Eds.) pp 67–81, de Gruyter, Berlin and New York.

Jaenicke, R. (1983b) *Naturwissenschaften 70*, 332–341.

Jaenicke, R. (1984) *Angew. Chem., Int. Ed. Engl. 23*, 395–413.

Jaenicke, R., & Perham, R. N. (1982) *Biochemistry 21*, 3378–3385.

Jaenicke, R., & Rudolph, R. (1983) *Colloq. Ges. Biol. Chem. 34*, 62–90.

Jaenicke, R., Rudolph, R., & Heider, I. (1979) *Biochemistry 18*, 1217–1223.

Jaenicke, R., Krebs, H., Rudolph, R., & Woenckhaus, C. (1980) *Proc. Natl. Acad. Sci. U.S.A. 77*, 1966–1969.

Kirschner, K., Wiskocil, R. L., Foehn, M., & Rezeau, L. (1975) *Eur. J. Biochem. 60*, 513–523.

Ko, B. P. N., Yazgan, A., Yeagle, P. L., Lottich, S. C., & Henkens, R. W. (1977) *Biochemistry 16*, 1720–1725.

Müller, K., Lüdemann, H.-D., & Jaenicke, R. (1982) *Biophys. Chem. 16*, 1–7.

Neumann, R. C., Jr., Kauzmann, W., & Zipp, A. (1973) *J. Phys. Chem. 77*, 2687–2691.

Paul, C., Kirschner, K., & Haenisch, G. (1980) *Anal. Biochem. 101*, 442–448.

Rudolph, R., Heider, I., & Jaenicke, R. (1977) *Biochemistry 16*, 5527–5531.

Schade, B. C., Rudolph, R., Lüdemann, H.-D., & Jaenicke, R. (1980) *Biochemistry 19*, 1121–1126.

Schmid, G., Lüdemann, H.-D., & Jaenicke, R. (1978) *Eur. J. Biochem. 86*, 219–224.

Seifert, T. (1980) Thesis, Regensburg University.

Seifert, T. (1983) Dissertation, Regensburg University.

Seifert, T., Bartholmes, P., & Jaenicke, R. (1982) *Biophys. Chem. 15*, 1–8.

Seifert, T., Bartholmes, P., & Jaenicke, R. (1984a) *Z. Naturforsch., C: Biosci. 39C*, 1008–1011.

Seifert, T., Bartholmes, P., & Jaenicke, R. (1984b) *FEBS Lett. 173*, 381–384.

Weaver, D. L. (1982) *Biopolymers 21*, 1275–1300.

Weischet, W. O., & Kirschner, K. (1976) *Eur. J. Biochem. 65*, 375-385.
Wiesinger, H., Bartholmes, P., & Hinz, H.-J. (1979) *Biochemistry 10*, 1979-1984.
Wilson, D. A., & Crawford, I. P. (1965) *J. Biol. Chem. 240*, 4801-4808.
Zabori, S., Rudolph, R., & Jaenicke, R. (1980) *Z. Naturforsch., C: Biosci. 35C*, 999-1004.
Zetina, C. R., & Goldberg, M. E. (1980) *J. Mol. Biol. 137*, 401-414.
Zettlmeissl, G., Rudolph, R., & Jaenicke, R. (1979) *Biochemistry 18*, 5567-5571.

Decrease in ADP-Ribosylation of HeLa Non-Histone Proteins from Interphase to Metaphase†

Kenneth W. Adolph* and Min-Kyung H. Song‡

Department of Biochemistry, The University of Minnesota Medical School, Minneapolis, Minnesota 55455
Received July 2, 1984

ABSTRACT: Variations for non-histones in the ADP-ribosylating activities of interphase and metaphase cells were investigated. ^{32}P-Labeled nicotinamide adenine dinucleotide ([^{32}P]NAD), the specific precursor for the modification, was used to radioactively label proteins. Permeabilized interphase and mitotic cells, as well as isolated nuclei and chromosomes, were incubated with the label. One-dimensional and two-dimensional gels of the proteins of total nuclei and chromatin labeled with [^{32}P]NAD showed more than 100 modified species. Changing the labeling conditions resulted in generally similar patterns of modified proteins, though the overall levels of incorporation and the distributions of label among species were significantly affected. A less complex pattern was found for nuclear scaffolds. The major ADP-ribosylated proteins included the lamins and poly(ADP-ribose) polymerase. Inhibitors of ADP-ribosylation were effective in preventing the incorporation of label by most non-histones. Snake venom phosphodiesterase readily removed protein-bound ^{32}P radioactivity. A fundamentally different distribution of label from that of interphase nuclei and chromatin was found for metaphase chromosome non-histones. Instead of 100 or more species, the only major acceptor of label was poly(ADP-ribose) polymerase. This profound change during mitosis may indicate a structural role for ADP-ribosylation of non-histone proteins.

Posttranslational modification of nuclear proteins by ADP-ribosylation is being increasingly recognized as having a significant role in the regulation of nuclear function (Hilz & Stone, 1976; Hayaishi & Ueda, 1977; Purnell et al., 1980; Smulson & Sugimura, 1980). In particular, ADP-ribosylation has been implicated in the control of gene expression and cell differentiation (Farzaneh et al., 1982; Althaus et al., 1982). A related role is in the repair of DNA damage caused by X-rays, ultraviolet light, and chemical carcinogens (Borek et al., 1984). The enzyme responsible for the synthesis of protein-bound poly(ADP-ribose), poly(ADP-ribose) polymerase, is tightly associated with chromatin (Chambon et al., 1966; Hasegawa et al., 1967; Nishizuka et al., 1967), and the histones are themselves major acceptors of poly(ADP-ribose) (Adamietz et al., 1978; Braeuer et al., 1981; Riquelme et al., 1979; Ogata et al., 1980a,b; Smith & Stocken, 1975; Wong et al., 1983; Burzio et al., 1979). Because of such evidence that ADP-ribosylation is an important posttranslational modification of nuclear proteins, this investigation was undertaken to determine basic differences in the ADP-ribosylation of non-histone proteins from interphase nuclei and metaphase chromosomes. ADP-ribosylation of non-histones had not previously been well characterized, and so an assessment of the solution conditions to investigate the modification with radioactive isotopes was required. In addition to metaphase chromosomes, the experiments focused upon the two major components of the interphase nucleus: chromatin and the nuclear scaffold (the protein framework of the nucleus, similar to the nuclear matrix). The ultimate aim of these studies is to relate cell cycle changes in ADP-ribosylation of non-histones to changes in the structural organization of the HeLa genome.

Previous cell cycle studies of the ADP-ribosylation of nuclear proteins were concerned with the levels of ADP-ribosylation at different phases of the cell cycle and with the state of modification of poly(ADP-ribose) polymerase. These reports did not emphasize variations in the modification of non-histones. For example, an antibody specific for poly(ADP-ribose) revealed peaks at mid-S and S/G_2 phases (Kidwell & Mage, 1976), and immunofluorescence techniques demonstrated the in situ presence of poly(ADP-ribose) for interphase HeLa cells and metaphase chromosomes (Kanai et al., 1981). Metaphase proteins showed the greatest degree of modification with an in vitro system of HeLa nuclei (Tanuma et al., 1978), and measurements of the level of modification showed a 4-5 times higher level in metaphase (Holtlund et al., 1983). Furthermore, poly(ADP-ribose) polymerase was present in an active form on metaphase chromosomes (Holtlund et al., 1980).

No investigations of ADP-ribosylation have been concerned with the structural protein framework of the nucleus (the nuclear scaffold or nuclear matrix), but reports on the modification of chromatin-associated proteins have appeared. In particular, modifications of the histones and poly(ADP-ribose) polymerase, considered to be a non-histone protein, have received considerable research attention. For chromatin fibers,

† This research was supported by a grant from the Graduate School of The University of Minnesota, by a Biomedical Research Support Grant of The University of Minnesota Medical School, and by Grant GM26440 from the National Institutes of Health.
‡ Present address: Laboratory of Carcinogen Metabolism, National Cancer Institute, National Institutes of Health, Bethesda, MD 20205.

0006-2960/85/0424-0345$01.50/0